EVS24
Stavanger, Norway, May 13-16, 2009

Influence of cathodes technology on the power capability and charge acceptance of lithium ion batteries.

Michael A. Roscher[1*], Jens Vetter[2], Dirk Uwe Sauer[1]

[1] RWTH Aachen University, Electrochemical Energy Conversion and Storage Systems Group, Institute for Power Electronics and Electrical Drives (ISEA), Jaegerstr. 17/19, 52066 Aachen, Germany,
E-mail: michael.roscher@rwth-aachen.de
[2] BMW AG, 80788 München, Germany
[*] Corresponding author

Abstract

Lithium ion cells (Li-ion) comprising lithium iron phosphate (LiFePO4) based cathode active material are a promising battery technology for future hybrid and electric vehicle applications in terms of safety, cycle and calendar lifetime and cost. Those cells comprise flat open circuit voltage characteristic and a long-term load history dependent cell impedance. In this work the special electric characteristics of LiFePO4 based cells are elucidated, quantified and compared to Li-ion cells containing competing cathode technologies. Through pulse tests and partial cycle tests, performed with various olivine based cells, the cycling history dependency of the internal resistance and therefore on the power capability is show. Hence, methods are illustrated to quantify this load history impact on the cells performance. Subsequently, methods to achieve a safe battery operation are elucidated. Furthermore strategies are given to obtain reliable information about the cells power capability, taking the mentioned properties into consideration.

Keywords: secondary battery, power, energy, HEV (hybrid electric vehicle), BEV (battery electric vehicle)

1 Introduction

The growing market for portable consumer electronics, e.g. cellular phones, cameras and portable computers, generates a need for large-scale producible, high potential energy storage devices. For this type of applications lithium ion batteries (Li-ion) became the favourable choice in the recent years, due to their increased energy density and power density in comparison to the former predominant nickel hydride batteries (NiMH) by a factor of two.

In nowadays commercial hybrid electric vehicles (HEV) the NiMH technology is still dominate (e.g. Toyota Prius, Lexus GS450h, Honda Insight Hybrid, etc.). For such very high power consuming and safety sensitive applications the market entry of Li-ion is still pending, but on the way. The introduction of new generation battery electric vehicles (BEV) got much public and media attention because of their not typical green vehicle design on the one hand and the usage of Li-ion batteries on the other hand. Although these cars are produced and sold in small numbers only, they opened the door for the large-scale introduction of Li-ion powered cars.

On this way some important challenges still have to be overcome. Especially safety and lifetime issues are the focus of further research. In recent

years, inventions are made referring to new production methods and materials, this stepwise improved the properties of modern Li-ion cells according to their lifetime stability and electrical characteristics. Additionally, the production costs for certain cells could be significantly decreased because of the introduction of more effective production techniques and the economics of scale.
In the course of the investigations on new electrode materials the iron based olivine type cathodes (mainly lithium iron phosphate, $LiFePO_4$) were identified as possible and quite promising alternatives to cathodes based on rare metal composites (i.e. the transition metal oxides $LiCoO_2$, $LiNiO_2$) [1, 2]. Among the resulting positive cost factor such cathodes are intrinsically safe and show a very good cycle life [3]. Unfortunately, cells containing these olivine cathodes have a reduced nominal voltage in comparison to competing Li-ion cells and thus have a slightly reduced energy density. Additionally, it is known that these cells show very special electrical properties according to their open circuit voltage (OCV) characteristics.

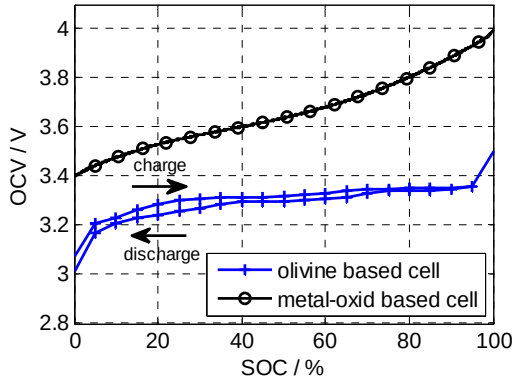

Figure 1: OCV of olivine based and metal oxide based cells (3h rest period at each SOC step).

Figure 1 gives an illustration of the differences between the OCV of a metal oxide and an olivine based cell. The OCV's are plotted versus the state-of-charge (SOC), normalized to the nominal capacity (completely charged cell → SOC = 100 %). As visible, the OCV of the olivine cell shows slight changes only with varying SOC and exhibits a kind of voltage hysteresis. Such hysteresis effects are well known from NiMH batteries [4] and were documented for Li-ion cells also [5]. It is obvious that from this OCV characteristic (slight gradient and hysteresis) certain challenges in terms of the SOC estimation in a device or application can arise.

2 Overview to the interaction between two-phase intercalation and OCV characteristics of olivine based Li-ion cells

The special OCV trait of the olivine based cells is closely related to the type of lithium intercalation/deintercalation process occurring within the cathode material. The lithium insertion or extraction, respectively, proceeds as a first order phase transition [6]. That means, two distinct phase regions develop (lithium rich and lithium poor phase) in one certain electrode out of an originally homogenous material. The two phases have different but constant lithium concentrations c_{Li} while the intercalation proceeds. This two-phase transition occurs over a wide range of SOC, hence occurs over a wide range of lithium concentration within the cathode [7, 8]. If one phase region grows, the barrier between the phases propagates within the solid material. The shift of a phase barrier is illustrated in figure 2a for the Li insertion in a thin film electrode model (1 dimensional model).
The phase barrier propagates from the electrodes surface toward the collector foil on the opposite site. As the intercalation/deintercalation is stopped and the current flow direction is inverted a new phase region emerges at the electrodes surface and the barrier starts to propagate toward the collector again (figure 2b). These phases are energetic favourable states of the host lattices. Hence, the phases do not mix and the barrier does not vanish, until the cathode is completely transformed. This means, during a complete charge process (Li deintercalation) the Li-poor phase is in touch with the electrolyte. On the other hand there is the Li-rich phase situated close to the electrolyte during the discharge process. This is the case for thin film cathodes as well as for porous electrodes [4].
The open circuit voltage is closely related to the electrode potential of the electrodes assembled in a certain battery cell. Thus, the olivine cathode has an almost constant open circuit voltage during discharge as well as during charge. Additionally, existence of different surface materials can be a feasible explanation for the occurrence of the OCV hysteresis effect.

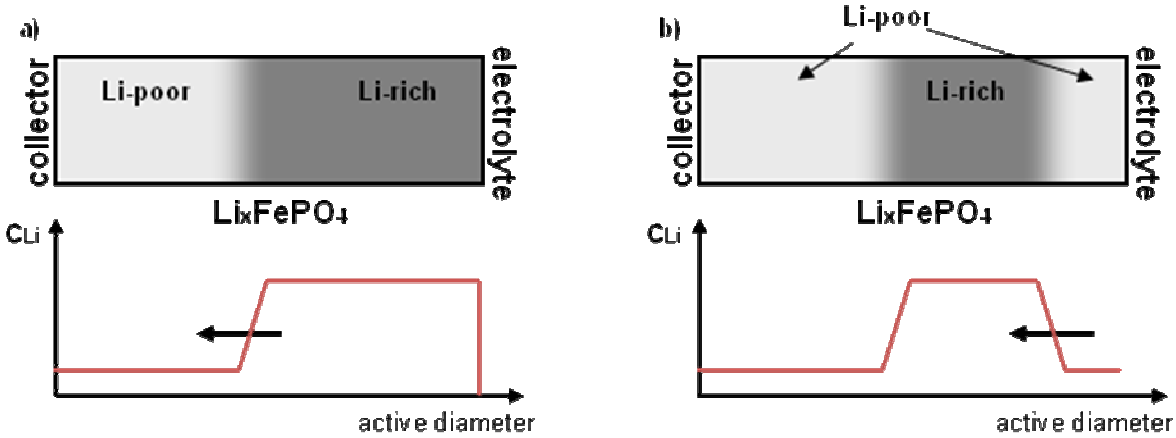

Figure 2: 1-D model of two-phase transition electrode and the specific lithium concentration profile during Li insertion and subsequent Li extraction.

3 Path dependency of the power and available capacity

3.1 Theoretical background and origin

The two-phase transition process and the resulting development of distinct phase regions is influencing the electrical characteristics of olivine based cells. Especially in case of the development of complex phase region sequences the diffusion electrode model [9] would not be a sufficient approach for modelling issues. It is evident that the thickness of the electrolyte nearest phase region has a strong influence on the diffusive voltage drop during intercalation/deintercalation. If this outermost region is Li-rich the extraction of lithium from this phase layer is easy and would cause a small overvoltage only, in comparison to the case of the outermost phase being Li-poor. In this case the diffusion path is longer for the lithium to get oxidised at the electrodes surface, thus, the diffusive voltage drop is higher during load. For the Li insertion this fact would be analogue, but with changed phases [10].

Another influencing factor on the electrical performance of Li-ion cell is the contacting of the active material to the collectors. Most electrodes are composites consisting of the active material itself, a conductive additive (mainly carbon) and a binder [11, 12]. The active material is milled to achieve small particles in order to achieve a high electrode surface and small diffusion lengths. The active particles of such a porous electrode are not completely coated with carbon. The particles have electrical contact to the collector at a few contact points only. Most of the particle surface is in direct contact to the electrolyte. At this surface the redox reaction between the Li ions and the electrons proceeds. The electrons come from the collector and the Li ions come from electrolyte (intercalation case). The conductivity for electrons within the active cathode material is low, consequently the reaction starts near the contact point, where ions and electrons meet. As more and more Li-poor material is transformed to Li-rich phase material the distances the electrons have to cover within the particles are increasing. This movement of the electrons causes voltage drops during current flow (ohmic resistance). This ohmic resistance is stable over time as the phases within the active cathode material are stable, too [13].

For cells designed for high energy densities the two mentioned aspect (diffusion path elongation and as a result the changing surface resistance) are expected to have more influence on the electric characteristics in comparison to power cells containing smaller particles and/or a higher content of contacting carbon. The following sections will give evidence that these two factors influence the electrical characteristics of olivine based cells in a relevant way.

3.2 The cells under investigation, tests being performed and the used test equipment

In order to get comprehensive information about the influence of the load history on the electrical characteristics of olivine based cells three different types of such cells were tested (two high energy cells with different geometries (cylindrical and prismatic) but sourced from the same vendor and one high power prototype cell from another vendor). To outline the different behaviors of cells containing various cathode materials a metal oxide based high energy cell type was tested, too.

A test schedule was developed incorporating charge/discharge tests and pulse power tests. The preconditioning prior to a certain test was equal for of the various cell types but was varied from test to test, especially the direction from which a certain SOC was adjusted (from the full or the empty state).
The tests were done on a Scienlab test bench. The cell voltages and currents were measured with a 24 bit analogue-digital-converters (accuracy: 0.25 % of the measured value ±1 mV) and LEM current sensors (accuracy: 0.25 % of the measured value ±30 mA in a range of –30 to 30 A and 0.25 % of the measured value ±600 mA for higher currents, respectively), integrated to the test bench. During some of the tests the cells temperatures were detected with Ni-CrNi thermal couples (temperature resolution and accuracy: ± 1 K). The couples were pasted to the cells cases.

3.3. Charge history dependent power capability

In repeated pulse sequences the different cell types are tested with shallow constant voltage charge periods and discharge periods, respectively. The pulses are performed with different starting SOC, scheduled as follows:

- CCCV
- 20% CC-discharge of nominal capacity
- 30 min zero current rest period
- 20 s charge or discharge CV pulse (cutoff voltage)
- etc.

After reaching the discharge cutoff voltage during CC discharge the cells are charged to SOC = 20% again. Subsequently, another pulse test is done and the cells are charged to SOC = 40% and so on. In this way current profiles can be obtained for SOC = 20 %, 40 %, 60 %, 80 % with the SOC being adjusted through discharge and charge, as well. To outline the specific behaviors figure 3 gives typical current discharge profiles (2.2 V) for the prismatic olivine based energy cells (at room temperature) after SOC adjustment through discharge and charge, respectively, with the currents being normalized to the cells nominal capacity (C-rate). The specific starting SOC of each pulse is given beneath the profiles. Figure 4 gives the equivalent profiles for the metal oxide based cell (2.5 V). As visible in the shown diagrams, for the olivine cells the available discharge current strongly depends on the way the SOC is reached. After charging the discharge current is nearly independent of the SOC. After discharge the currents significantly differ. The available current of the metal oxide cells is quite independent of the charge history but is closely correlated to the SOC, in contrast.

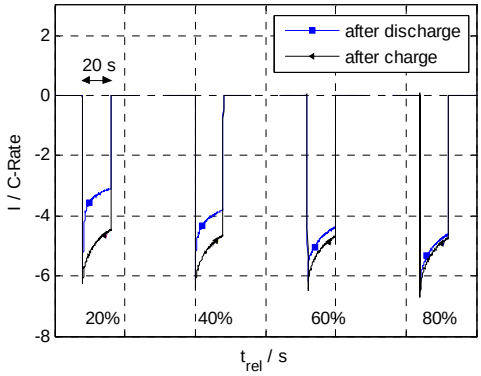

Figure 3: Current profiles during 2.2 V CV discharge of the prismatic olivine based cells.

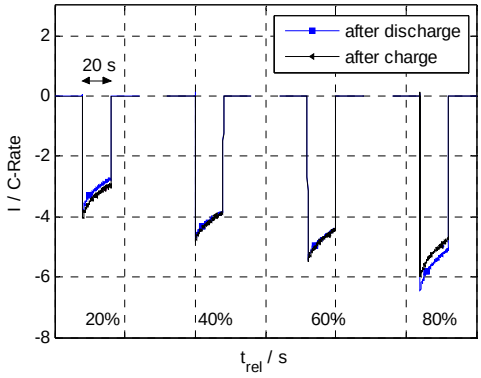

Figure 4: Current profiles during 2.5 V CV discharge of the metal oxide cells.

This behavior cannot be assigned to the OCV hysteresis alone. In a rough calculation for the shown case (figure 3): 2.2 V constant voltage discharge of an olivine energy cell at SOC = 20 %, the OCV prior to the pulse is 3.35 V after charge and 3.3 V after discharge. Hence, the voltage differences to the cutoff voltage differ less than 5 % (1.15 V ↔ 1.1 V). However, the measured currents differ more than 30 % during the pulse duration. This indicates a changed internal resistance superimposing the OCV hysteresis effect and having a much stronger impact on the power capability.
A comprehensive overview of the pulse currents measured during the constant voltage tests is given in table 1 for the four investigated cell types. The currents are given for the distinct pulse

Table 1: Normalized pulse currents (charge and discharge) for various pulse periods with various SOC (currents after discharge/charge SOC adjustment; all current given with positive signs).

SOC (%)	$I_{dis,1s}$ (C)	$I_{dis,20s}$ (C)	$I_{cha,1s}$ (C)	$I_{cha,20s}$ (C)	SOC (%)	$I_{dis,1s}$ (C)	$I_{dis,20s}$ (C)	$I_{cha,1s}$ (C)	$I_{cha,20s}$ (C)
olivine based cylindrical energy cell					olivine based prismatic energy cell				
20	3.4/3.8	2.6/3.1	1.8/1.7	1.6/1.5	20	4.3/5.7	3.1/4.5	2.8/2.7	2.5/2.3
40	3.6/3.9	2.9/3.2	1.7/1.7	1.5/1.4	40	4.9/5.9	3.8/4.7	2.6/2.6	2.4/2.1
60	3.8/3.9	3.1/3.2	1.7/1.6	1.5/1.3	60	5.5/6	4.4/4.7	2.6/2.5	2.3/1.4
80	3.8/4	3.1/3.2	1.6/1.6	1.4/0.9	80	5.9/6.2	4.6/4.7	2.5/2.4	2.2/0.9
olivine based prototype power cell					metal oxide based reference energy cell				
20	39.1/47.3	15.9/19.3	27.2/28	20.2/20.8	20	3.8/3.8	2.6/2.7	3.7/3.4	3.3/3.2
40	45.5/52	26.2/32.8	25/25.1	19.8/18.9	40	4.7/4.7	3.9/3.9	3.6/3.3	3.3/3
60	48.1/53.4	31.7/37.3	24.9/24.5	18.2/16.5	60	5.4/5.4	4.3/4.3	3.4/3.1	2.9/2.8
80	51.3/56.3	36.5/40.5	22.5/22	14.4/12	80	6.1/5.8	5.2/4.8	2.8/2.7	2.4/2.1

durations t = 1 s and t = 20 s. The cutoff voltages were chosen as follows:

- olivine energy cells: 3.8 V charge / 2.2 V discharge
- olivine power cells: 3.7 V charge / 2.6 V discharge
- metal oxide cells: 4.2 V charge / 2.5 V discharge

The voltage limits for the power cells were chosen more conservative in order to prevent currents exceeding the allowed limits specified by the manufacturer.

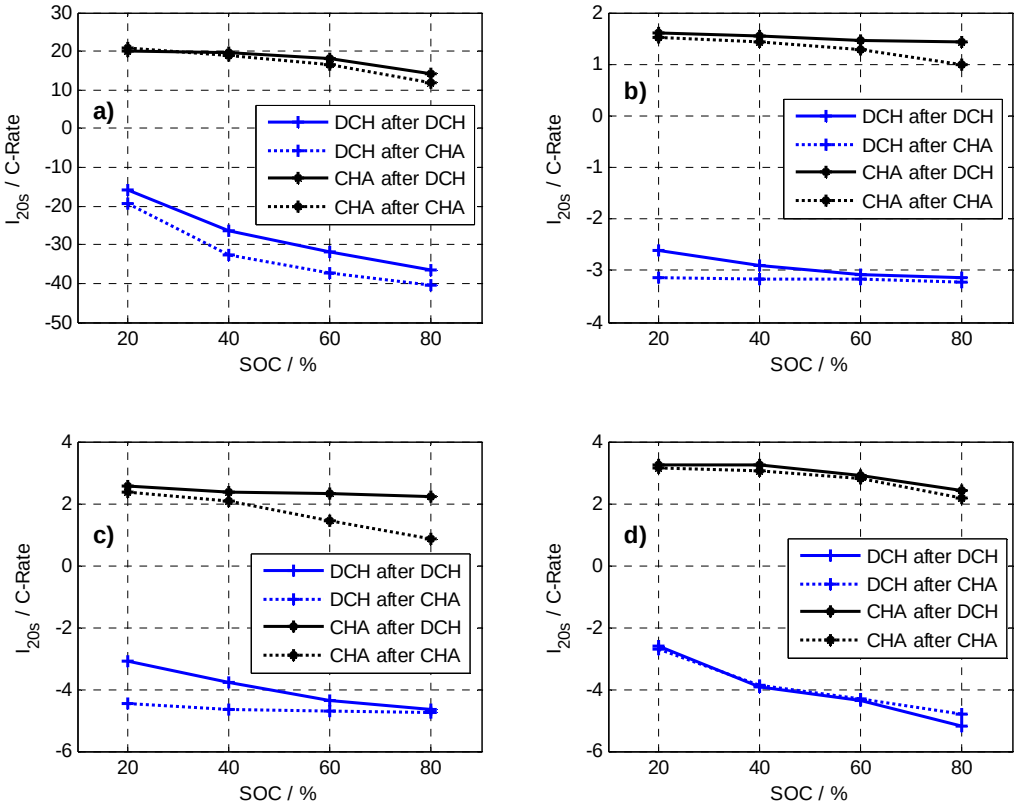

Figure 5: 20s charge and discharge currents at various SOC for olivine based power cells (a), cylindrical energy cells (b), prismatic energy cells (c) and metal oxide based energy cells (d).

The measurement results show that the path dependence of the pulse current capability of olivine based cells increases as the SOC reaches the boundary regions (very high, very low SOC). With the variance of the currents (after charge SOC adjustment in comparison to discharge SOC adjustment) in most cases being less than 10% in the mid SOC region, these differences may rise to over 30% for discharge currents as the SOC is decreased and rises to more than 70% for the charge currents as the SOC increases, respectively.
The power cells do not show such drastic influence of the charge history on their power capability. These cells show a stronger influence of SOC on the available power, which is significant for the reference (metal oxide) cells, but is different to the behavior of the two olivine-based energy cell types, as visible in figure 5.

3.4. Charge history dependent available capacity

If the internal resistance varies according to the SOC adjustment, also an influence on the available capacity is expected, due to the cutoff voltage value during charge / discharge cycling is expected to be reached earlier or even later, respectively. In order to investigate this hypothesis, partial cycle tests (complete charge or complete discharge) are done, beginning in the medium SOC range. For this purpose the olivine based prismatic energy cells and the high power prototype cells underwent these tests.

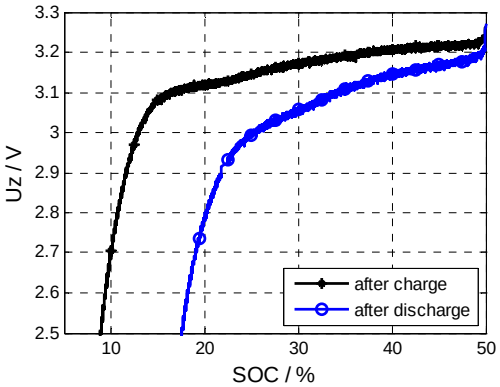

Figure 6: Voltage profiles during discharge of prismatic olivine based cells (0.3 C-rate current).

Figure 6 gives the typical cell voltage of the energy cells during a 0.3 C discharge. The initial SOC was adjusted to 50 %, first time through discharging of a completely charged cell and the second time by charging of an empty cell. The discharge current stops as a voltage of 2.5 V is reached. The differences between the two curves are obvious, indicating different internal resistances of the same cell, originating from the way the SOC was adjusted only. Hence, it is evident that the load history has a strong impact on the short time internal resistance (pulse tests in section 2.3.) as well as on the long term resistance.

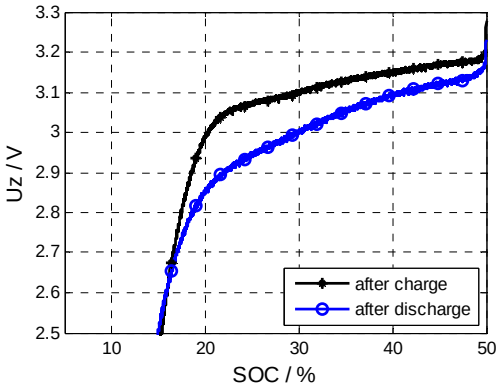

Figure 7: Voltage profiles during discharge of prismatic olivine based cells (0.5 C-rate current).

Figure 7 gives the voltages during the same tests, but with a discharge rate of 0.5 C.
During most time of the discharge period the differences are similar to the curves during the 0.3 C discharge tests. As the voltages are decreasing due to the decreasing OCV in this range, the voltage gap between the curves decreases, too. In our opinion, this effect correlates to the difference in the internal power losses resulting in an unequal self heating of the cells. Actually, the measured cell temperatures at the end of each 0.5 C test differ approximately 7 K.
The internal warming leads to an enhanced conductivity of the active material. Hence, the overvoltage decreases, subsequently the available capacity increases. Surprisingly, this leads to a higher usable discharge capacity for a 0.5 C discharge compared to 0.3 C discharge rate, if the SOC = 50 % is adjusted by discharging of a completely charged prismatic energy cell.
Table 2 gives an overview on the available charge and discharge capacities of olivine based cells at a SOC of 50%, at room temperature. The given percentages are the SOC values of the cells as they are reaching the distinct cutoff voltages.
For the energy cells the SOC history dependency is much stronger than for the power cells. For the discharge test of the power cells the effect of crossing voltage curves caused by self heating was measured again (comparable to figure 7).

Table 2: Remaining SOC when hitting the cutoff voltage of olivine based prismatic energy cells and power cells, depending on the SOC sequence.

Cycle SOC steps	energy cell			power cell			
	cutoff	current		cutoff	current		
		0.3 C	0.5 C		1 C	3 C	10 C
0 → 50 →100	3.5 V	75 %	63 %	3.6 V	98.5 %	92.5 %	76 %
100 → 50 →100	3.5 V	95 %	88 %	3.6 V	99 %	95.5 %	87 %
0 → 50 → 0	2.5 V	8 %	15 %	2.5 V	-5 %	-3.5 %	-1 %
100 → 50 → 0	2.5 V	17 %	15 %	2.5 V	-5 %	-3 %	-2.5 %

According to that, this effect is assigned to be a general property of olivine based cells.

3.5. SOC memory behavior

In the previous sections the initial SOC was adjusted on one hand by discharging a full cell, on the other hand through charging of an empty cell. In a subsequent test the voltage response after a SOC adjustment including intermediate steps with a change in the current direction was investigated. Thus, an SOC = 40 % was adjusted in two ways, in a charge dominated load cycle 1 (SOC = 0 % → 60 % → 40 %) and a discharge dominated cycle 2 (SOC = 100 % → 40%). Both times the cells were discharged right before reaching the target SOC = 40 %. Cycle 2 is similar to the load regimes in section 2.4.
Typical voltage responses for 3 C charge of the power cells are shown in figure 8 (SOC sequences are given in the legend). Figure 9 depicts the voltages during the same test of the prismatic energy cells during a 0.3 C load.

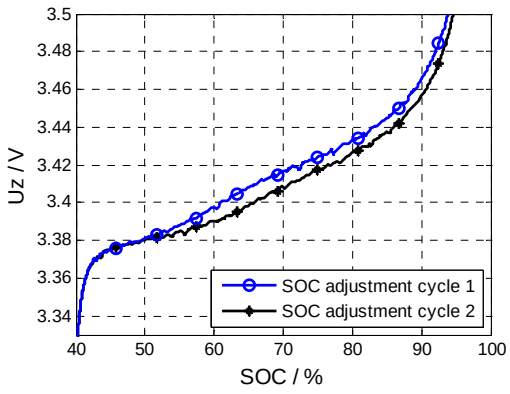

Figure 8: Voltage during CC charge (3 C) of olivine based power cells.

Right after the beginning of the charge section the voltages after both SOC adjustment cycles are quite similar. As a SOC of approximately 50 % is reached a voltage difference arises and consequently increases. For the power cells a maximum voltage gap is reached at a SOC ≈ 65 %. After that the voltage gap remains nearly constant. For the energy cells the voltage difference increases more and more as the SOC increases, too. A maximum cannot be found, before the cells are reaching the cutoff voltage.

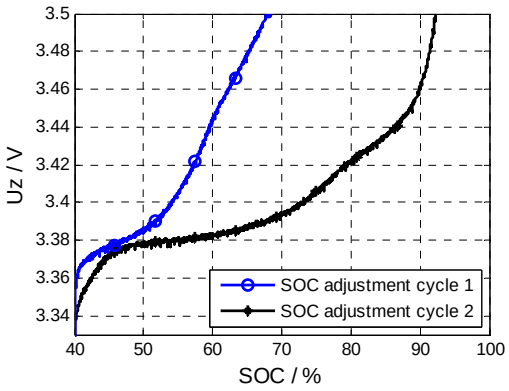

Figure 9: Voltage during CC charge (0.3 C) of prismatic olivine based cells.

To visualize this fact figure 10 gives a plot of the voltage differences divided by the normalized currents for both cells types ($\Delta R^* = (U_{cycle1} - U_{cycle2}) * C\text{-}rate^{-1}$), for the charge case of the power cells (figure 10a) and the energy cells (figure 10b). The rise of the internal resistances starts at a SOC of approx. 50 % for both of the investigated cells, as described above. The maximum resistances change of the power cells can be identified at SOC = 63 %, at higher SOC the ΔR^* slightly decreases and rises again as the cells are becoming completely charged. A comprehensive theory explaining this matter is not yet available. One possible reason might be again the different self heating, which leads to an increasing conductivity of the contactors and the electrolyte. The internal resistance rise of the prismatic energy cells continues in a linear way, in contrast to the power cells.
A more detailed investigation and description on this load history memory topic of olivine based power cells is outlined in another paper [14] published from our research group.

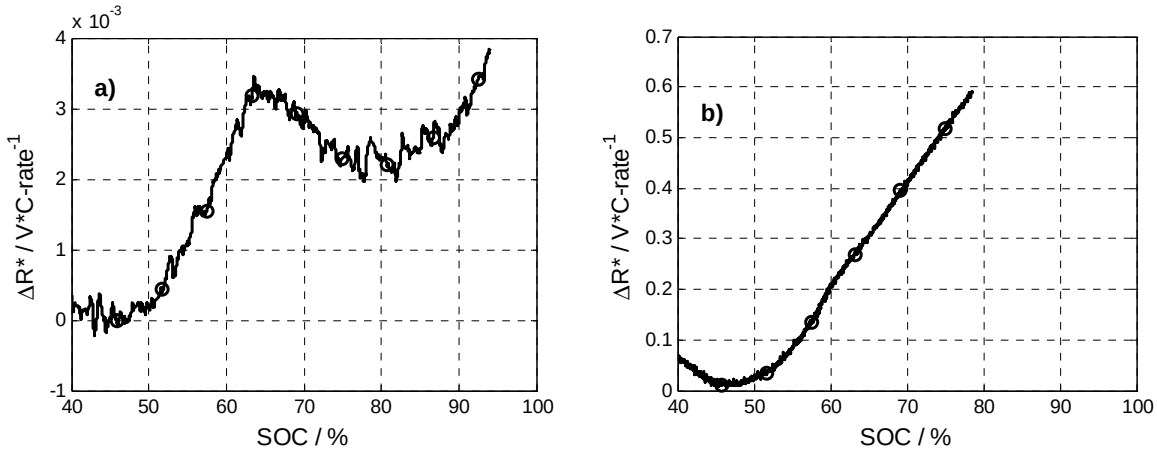

Figure 10: Illustration of ΔR* for olivine based power cells (a) and prismatic energy cells (b).

4 Discussion and model approach

4.1 Consequences in applications

The sections above gave a qualitative and quantitative overview in which way the charge/discharge history, especially the SOC sequence, influences the power capability and available capacity of olivine based cells. Therefore, the results outlined in sections 2.3 and 2.4 are a comparison of the best to the worst possible load cases for cells in an application. Fortunately, these artificial test cases, including full charge and complete discharge, are not typical operating conditions. In HEV systems the operation windows would be defined much smaller (e.g. SOC = 30…60%), according to power requirements, cold cranking and aging issues. In BEV applications the operation window may be extended to SOC = 0…100 %, but the cells are mainly discharged during drive cycles. This means a SOC of 80 % is seldom reached through regeneration starting form SOC = 0 %, for example. During the charge phases (i.e. connected to grid for several hours) the power and capacity differences caused by changed internal resistances can be neglected, due to the long charge periods.

However, during full cycle tests or typical parameterization test schedules (FreedomCAR [15], HPPC from the PNGV [16]) the cells undergo the best or the worst load case, respectively. Hence, if the results from such test are used for power prognosis jobs in battery management systems, in most cases the available power will be under- or even overestimated. Underestimation is not critical, the storage system is always able to supply the predicted power, but this would reduce the systems utilization. Overestimation can result in hitting or exceeding the cells voltage and/or current limits during a power controlled load section. This may lead to dangerous storage temperatures, a reduced calendar life or to an irreversible damage of the storage system.

4.2. Power prognosis approaches

As a simple method to prevent any dangerous battery states caused by a wrong power prediction would be the introduction of voltage und current buffers to reduce the usable operation window of the cells, hence, to prevent the exceeding of the limits, even if the predicted power is served to or taken from the battery system. Due to the results from pulse tests in section 2.3 the buffers have to be dimensioned carefully. If the buffers are dimensioned in a way that the cell limits are not violated, even in the SOC boundary regions, the power capability utilization would be reduced about 30…50 % over the entire SOC range.

Another method would be a conservative parameterization. All set points for power maps are carried out by worst case measurements (charge tests after charge dominant SOC adjustment and discharge tests after discharge dominant SOC adjustment, respectively). In contrast to the method outlined before, the system utilization would be better in the mid SOC region, but in most cases the predicted power is significant lower than the power the storage system can actually supply. This would still not be tolerable for high power application like HEV applications.

If a rigorous prognosis method is required, the load history has to be taken into account when predicting power and available energy. A possible approach can be deviated from the mechanisms explained in section 2.1 of this work. The growth

of an ohmic and diffusive phase resistance R_{ph} (in addition the cells impedance) resulting from phase growth is an easy to handle battery state resulting from counting the charge throughput within the cells. To sum up the monotonously flown current with a resettable integrator (reset if the current direction toggles) is a feasible way to track this internal state. A scaling factor which correlates the current integral value to R_{ph} can be deviated from measurements similar to those explained in section 2.4. The power prognosis itself can be done based on a typical batteries equivalent electric circuit using the OCV, the electrical cell limits (U_{cutoff}, I_{max}) and the batteries impedance [17].
This method works in a sufficient way for simple SOC sequences (test cases in sections 2.3 and 2.4). If the SOC sequence becomes more complex (test cases in section 2.5) the method has to be extended in a way that the electrodes inner phase regions are incorporated to the calculation of R_{ph}, too. A stack memory tracking all the virtual phase widths [14] would be an appropriate solution. To model the transition from a low resistance to a high resistance case (as visible in section 2.5 in the range SOC = 50…63 % for the voltage response after cycle 2), the knowledge of the virtual phase sequences is used, and in addition an empiric approach is implied to reproduce the ramped increase of R_{ph}.
Beside a model based power prognosis approach the usage of fuzzy logic systems or artificial neural networks using e.g. the OCV, the cell limits, and the information about the SOC sequence are possible solutions, but these techniques are not in the focus of this work.

4.3 Parameterization schedule suggestion for the virtual phase based power prediction method

It is evident that the strong SOC sequence influence on the power characteristic of olivine based cells makes necessary to carry out power results for both the best and the worst cases. That means discharge tests have to be done after the cells were discharged and after the cells were charged (analogue for the charge tests). It is not necessary to achieve results for cases between best and worst case, due to the introduction of the model parameter R_{ph}. A possible procedure for pulse tests would be as follows:

1. CCCV
2. SOC adjustment (discharge)
3. discharge pulse
4. rest period
5. charge pulse

(repeat steps 2.-5. until SOCmin)

6. SOC adjustment (charge)
7. charge pulse
8. rest period
9. discharge pulse

(repeat steps 6.-9. until SOCmax)

Test steps 3. and 7. are the worst case and steps 5. and 9. are the best case tests. This measurement is rigorous only if the SOC change during one pulse section can be neglected. Otherwise charge and discharge test cannot be carried out during the same test. Hence, it is obvious that a comprehensive pulse power characterization (over the complete temperature range and with different currents) alone needs a multiple of the time, compared to the HPPC or FreedomCAR tests. Furthermore, capacity tests are more complex, due to the starting SOC strongly influencing the capacity reserve. Partial cycle tests are required and tests to determine the R_{ph} transition (comparable to section 2.5) from a low resistive to a higher resistive case (the way around is not possible) are mandatory in order to achieve a comprehensive electrical characterization.

Conclusion

The intercalation process within olivine based cathode materials for Li-ion secondary cells differs from the intercalation mechanism proceeding within metal oxide based cathodes. During intercalation the development of distinct Li-rich and Li-poor phases occurs. The appearance of geometric separated phases within the solid cathodes has a strong influence on the electrical characteristic of olivine based cells. The power capability at different initial SOC is investigated and compared to metal based cells. The olivine based cells show a strong impact of the way the initial SOC was adjusted (not the SOC itself) on the power capability, in contrast to the metal oxide based reference cells. The charge power capability is much higher whether the SOC being adjusted through discharge than after a charge SOC adjustment. Analogue, the discharge power is higher after charge than after discharge. The SOC itself is less relevant.
Subsequently, a strong influence of the SOC adjustment way on the available capacity is identified. As expected from the power tests, the charge capacity is higher after discharge dominated SOC adjustment and vice versa. According to the obtained results a number of

applicable methods for the development of online power prognosis algorithms are outlined. A simple test schedule is introduced considering the need for a detailed characterization of the mentioned effects.
The aim of this work was to show that olivine based cells (mainly $LiFePO_4$ based cells) offer a number of challenges related to the development of reliable management strategies, beside the apparent advantages this technology offers in comparison to competing Li-ion technologies. It was shown that the typical and wide spread power and capacity test schedules would not generate all of the results, which would be necessary to obtain a comprehensive cell characterization.

References

[1] J. B. Goodenough, A. K. Padhi, K. S. Nanjundaswamy, C. Masquelier, U.S. Patent No. 5,910,382 (1999)

[2] A. K. Padhi, K. S. Nanjundaswamy, J. B. Goodenough, J. Electrochem. Soc. 144 (1997) 1188-1194

[3] K. Striebel, J. Shim, V. Srinivasan, J. Newman, *Comparison of LiFePO4 from different sources*, Lawrence Berkley National Laboratory – Paper LBNL55781, 2004

[4] V. Srinivasan, J. W. Weidner, J. Newman, J. Electrochem. Soc. 148 (2001), A969-A980

[5] J. Gerschler, D. U. Sauer, *Investigation of Open-Circuit-Voltage Behavior of Lithium-Ion Batteries with Various Cathode Materials under Special Consideration of Equilibrium Voltage Phenomena*, poster presentation at EVS 24, 2009

[6] N. Meethong, H.-Y. Shadow Huang, W. C. Carter, Y.-M. Chiang, Electrochem. Solid-State Lett. 10 (2007) 134-138

[7] M. Gaberscek, R. Dominko, J. Jamnik, J. Power Sources 174 (2008) 944-948

[8] V. Srinivasan, J. Newman, J. Electrochem. Soc. 151 (2004) 1517-1529

[9] F. L. Mantia, J. Vetter, P. Novák, Electrochim. Acta 53 (2008) 4109-4121

[10] V. Srinivasan, J. Newman, Electrochem. Solid-State Lett. 9 (2006) 110–114

[11] M. Winter, J. O. Besenhard, M. E. Spahr, P.Novák, Adv. Mater. 10 (1998) 725-763

[12] J. Shim, A. Guerfi, K. Zaghib, K. Striebel, *Effect of conductive additives in LiFePO4 cathode for lithium-ion batteries*, Lawrence Berkley National Laboratory – Paper LBNL54101, 2003

[13] K. Thomas-Alyea, 214th Meeting of the Electrochemical Society, 2008 (Abstract #2685)

[14] M. A. Roscher, J. Vetter, D. U. Sauer, J. Power Sources (2008), doi:10.1016/j.jpowsour.2009.02.024

[15] U.S. Department of Energy; *FreedomCAR Battery Test Manual For Power-Assist Hybrid Electric Vehicles*, DOE/ID-11069, 2003

[16] U.S. Department of Energy; *PNGV Battery Test Manual, Rev. 0*, DOE/ID-10597, 1997

[17] G. Plett, International Patent No. WO 2005/050810 A1 (2004)

Authors

Michael A. Roscher, Dipl.-Ing., RWTH Aachen University, Germany (michael.roscher@rwth-aachen.de).
M. A. Roscher received his diploma in Electrical Engineering from the Chemnitz University of Technology in 2007. Since 07/2007 he is PhD student at the RWTH Aachen in collaboration with the BMW Group.

Jens Vetter, Dr. rer. nat., BMW Group (jens.vetter@bmw.de).
J. Vetter received a PhD in Chemistry in 1999 from Stuttgart University, Germany. In 2000 he has been a research scientist at Aalen University. From 2000-2006 he worked at Paul Scherrer Institute, Switzerland, in the field of Li ion batteries. Since 2007 he is employed at BMW Group in Munich, Germany.

Dirk Uwe Sauer, Prof. Dr. rer. nat., ISEA, RWTH Aachen University, Germany (sr@isea.rwth-aachen.de).
D. U. Sauer received his diploma in Physics in 1994 from University of Darmstadt. From 1992-2003 he has been scientist at Fraunhofer Institute for Solar Energy Systems ISE in Freiburg/Germany. In 2003 he received his PhD at Ulm University on battery modeling and system optimization. Since 10/2003 he is Juniorprofessor at RWTH Aachen University for "Electrochemical Energy Conversion and Storage Systems"